Towards blended rational interpolation of multi-fidelity antenna data

Annie Cuyt* Ridalise Louw† Christophe Segers* Dirk de Villiers†

Abstract — **Over the past few years there is a clear trend towards design exploration using mathematical modelling. The data sets generated for this purpose may be huge and/or expensive. We describe how rational interpolation can be useful in this respect. In our exploration we focus on the univariate case, although all models can easily be generalized to a multivariate setting when the multivariate data sets are tensor (grid) structured. The example we include models the impedance of a pyramidal sinuous antenna.**

1 PROBLEM STATEMENT

1.1 Introduction

Log-periodic antennas have recently garnered renewed research interest since they found application as wideband reflector antenna feeds. The addition of a ground plane ensures a stable phase center in addition to the relatively frequency stable uni-directional (through relaxation of the self-complimentary constraint) radiation pattern [1, 2, 3]. Simulation of these structures through full-wave computational electromagnetic (CEM) solvers is normally computationally very expensive due to the inherent multi-scale features of the antenna and large frequency bandwidth.

In this paper we present a new rational interpolation scheme to significantly accelerate the input impedance modeling of non-self-complementary log-periodic antennas, specifically the pyramidal sinuous antenna of [3]. Multi-fidelity data is obtained by simulation of a truncated sinuous antenna, used as the low fidelity (LF) data, along with a similar full bandwidth antenna, used as the high fidelity (HF) data. Since the mid-band behavior of the impedance is expected to follow a roughly log-periodic frequency dependence, we are only interested in accurate models of the impedance at the band-edges. Since the truncated antenna becomes electrically smaller and better scaled due to the reduced bandwidth of the problem, the LF data are obtained from cheaper CEM simulation. A multi-fidelity rational interpolation scheme interpolates the frequency variation of sparsely sampled HF (full antenna) data from the more densely sampled LF data (truncated antenna).

1.2 Antenna description

The antenna used here is a pyramidal sinuous antenna as described in [3], and shown in Figure 1.

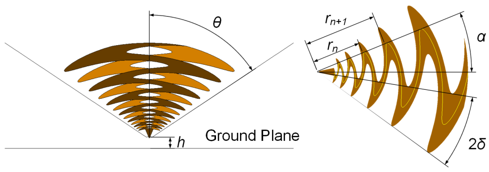

Figure 1: Pyramidal sinuous antenna.

Design parameters are τ, δ, α and θ, where $\tau = r_n/r_{n+1}$ is the growth rate ratio. Furthermore, the minimum and maximum values of the projected radius r_1 and r_N (where N is the total number of sinuous cells) are determined from the bandwidth as $r_1 = \lambda_H/[8(\alpha+\delta)]$ and $r_N = 1.2\lambda_L/[4(\alpha+\delta)]$ where λ_H and λ_L are the respective wavelengths at the high and low cutoff frequencies. We consider an antenna with an approximately 3:1 bandwidth (between 350 and 1050 MHz) as the HF model and a truncated antenna of 2:1 bandwidth (between 350 and 700 MHz) as the LF model. The design parameters in our example equal $\tau = 0.7825$, $\alpha = 22.5°$, $\delta = 13.5°$, $\theta = 53°$ and $h = 5$ mm. Note that, for the LF model, we only simulate the first half of the bandwidth (up to 525 MHz) in order to ignore the unwanted high frequency edge effect which is not physically related to the HF antenna model.

A comparison of the computational requirements for the two models is given in Table 1, with all simulations performed using the method of moments code FEKO. Even for this modest bandwidth design a significant speed-up by a factor of 5 is ob-

Model	Frequency (MHz)	Mesh (#triangles)	CPU time (hours)
Fine	350 - 1050	4869	5.819
Coarse	350 - 700	3477	1.217

Table 1: Comparison of fine and coarse models.

*Departement WIS-INF, Universiteit Antwerpen, Middelheimlaan 1, B-2020 Antwerpen, Belgium, e-mail: annie.cuyt@uantwerpen.be

†Electrical and electronic engineering, Stellenbosch University, Private Bag X1, Matieland 7602, South Africa, e-mail: ddv@sun.ac.za

served for the LF model evaluation. When the bandwidth of the HF model is increased, however, this improvement factor rapidly grows since the number of CEM unknowns in the HF model scales with bandwidth squared, while the LF model simulation time remains constant.

2 RATIONAL MODELLING SCHEME

2.1 Rational interpolation of HF data

Given data $f_i = f(x_i)$ at distinct points $x_i \in [a, b]$, a rational function $r_{n,m}(x)$ of degree n in the numerator and m in the denominator that interpolates these data is computed from

$$p(x) = \sum_{i=0}^{n} a_i x^i$$
$$q(x) = \sum_{i=0}^{m} b_i x^i$$
$$(fq - p)(x_i) = 0, \qquad i = 0, \ldots, n+m. \tag{1}$$

Since different solutions p_1, q_1 and p_2, q_2 of (1) are equivalent, meaning that $p_1(x)q_2(x) = q_1(x)p_2(x)$, the rational interpolant $r_{n,m}(x)$ is defined as the irreducible form of $p(x)/q(x)$ with p, q satisfying (1). Its representation can be normalized in different ways: one can prefer a monic numerator, or monic denominator or any other normalization. This choice is of no importance.

An advantage of working with rational functions is their ability to model steep changes and singularities. A drawback of the use of rational functions is of course the fact that they may exhibit undesirable poles. Moreover, when a zero of the denominator polynomial $q(x)$ occurs at an interpolation point x_i, then the interpolation condition at x_i may not be met, since the equation $(fq)(x_i) = p(x_i)$ implies that the same x_i is also a zero of the numerator. Hence condition (1) is satisfied whatever the value of f_i is. Such an interpolation point is called unattainable.

Our aim is to develop a model that is free from undesirable poles and unattainable interpolation points. To this end we introduce barycentric rational interpolation.

2.2 Barycentric interpolation of HF data

Let $\ell_i(x) = \prod_{j=0, j\neq i}^{n}(x - x_j) = \ell(x)/(x - x_i)$ where $\ell(x) = \prod_{j=0}^{n}(x - x_j)$ and let

$$r_{n,w_0,\ldots,w_n}(x) = \frac{\sum_{i=0}^{n} w_i f_i \ell_i(x)}{\sum_{i=0}^{n} w_i \ell_i(x)} = \frac{\sum_{i=0}^{n} w_i f_i/(x - x_i)}{\sum_{i=0}^{n} w_i/(x - x_i)}.$$

Then $r_{n,w_0,\ldots,w_n}(x)$ interpolates at the points $x_i, i = 0, \ldots, n$ for whatever w_i. While in the previous section both numerator and denominator were determined from $n+m+1$ interpolation conditions, here the denominator is fixed by the location of the x_i and the numerator guarantees the interpolation property. So the number of interpolation conditions is reduced to $n + 1$.

A necessary condition for $r_{n,w_0,\ldots,w_n}(x)$ to be polefree is $w_i w_{i+1} < 0$ [4]. For instance, it can be proven that the choice $w_i = (-1)^i$ guarantees a barycentric rational interpolant $r_{n,w_0,\ldots,w_n}(x)$ free of real poles. As a consequence no interpolation points can be unattainable. An example of this applied to the impedance Z of the antenna explained in Section 1, is shown in Figure 2.

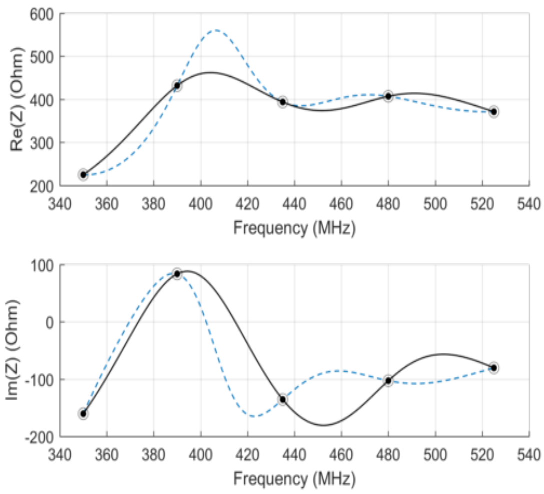

Figure 2: Barycentric interpolation applied to the real and imaginary parts of the impedance Z (circled dots: interpolation points, blue dashed line: validation values, black line: $r_{n,w_0,\ldots,w_n}(x)$ with $w_i = (-1)^i$).

A sufficient condition for weights $w_i = (-1)^i \omega_i$, with $\omega_i > 0$ and $a < x_0 < \ldots < x_n < b$, to guarantee a denominator free of poles on the real line [5], is given by

$$\begin{aligned} \frac{\omega_{j-1}}{b - x_{j-1}} &< \frac{\omega_j}{b - x_j}, \qquad j = 1, \ldots, n \\ \frac{\omega_j}{x_j - a} &> \frac{\omega_{j+1}}{x_{j+1} - a}, \qquad j = 0, \ldots, n-1. \end{aligned} \tag{2}$$

Remains to choose the w_i such that inbetween the high fidelity (HF) data that are being interpolated, the rational function follows a trend indicated by some low fidelity (LF) data.

2.3 Barycentric interpolation of multi-fidelity data

In order to distinguish between the HF and the LF data points, we denote the former by x_i^H and the latter by x_i^L. We also denote the values given at the points x_i^H by f_i^H and those given at x_i^L by f_i^L. The number of HF points is denoted by $n+1$ and that of LF points by $m+1$, so n and m get a different meaning compared to (1). The rational interpolant we are interested in now is the one given by

$$r_{n,w_0,\ldots,w_n}(x) = \frac{\sum_{i=0}^{n} w_i f_i^H/(x - x_i^H)}{\sum_{i=0}^{n} w_i/(x - x_i^H)} \tag{3}$$

where the w_i satisfying (2) are given by

$$\arg \min_{w_0,\ldots,w_n} \sum_{j=0}^{m} \left| f_j^L - r_{n,w_0,\ldots,w_n}(x_j^L) \right|^2 . \tag{4}$$

Condition (4) is a nonlinear optimization problem, which can be replaced by the linearized

$$\arg \min_{w_0,\ldots,w_n} \sum_{j=0}^{m} \left| f_j^L \sum_{i=0}^{n} w_i/(x_j^L - x_i^H) - \sum_{i=0}^{n} w_i f_i^H/(x_j^L - x_i^H) \right|^2 . \tag{5}$$

A similar approach, that however did not guarantee a polefree model, was presented in [6]. Although the formulas (3)-(4) or (3)-(5) express precisely what we expect from the computed rational model, the constraints (2) often restrict the search space for the least squares problems so much that the $w_0, \ldots, w_n$ resulting from the optimization problem do not deliver a really good model.

Figure 3 illustrates (3), with the constraints (2) and (5) applied.

So in practice, the method does not meet our expectations. This has encouraged us to look for yet another improvement.

2.4 Blended rational models for multi-fidelity data

We stick to the concept of the barycentric form which we want polefree, but preferably with a more relaxed condition than (2) on the weights in the expression. Therefore we turn our attention to blended models. Already the Lagrange form of a polynomial $p_n(x)$ of degree n, interpolating data f_i at points x_i for $i = 0, \ldots, n$,

$$p_n(x) = \sum_{i=0}^{n} w_i f_i \ell_i(x), \qquad w_i = 1/\prod_{j=0, j\neq i}^{n} (x_i - x_j),$$

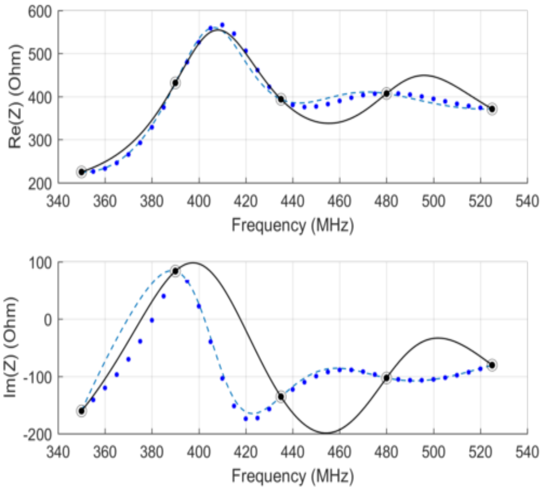

Figure 3: Interpolation of multi-fidelity data from (3) and (5) with (2) (circled dots: HF interpolation points, blue dots: LF data, blue dashed line: validation values, black line: rational model).

can be considered as a simple blended model: the local interpolants f_i at x_i are blended together into a global interpolant by the blending functions $\ell_i(x)$ which by the choice of appropriate weights evaluate to 1 at the x_i. We explain how this idea can be applied to our problem statement.

Let the x_i^H be indexed such that $x_0^H < \ldots < x_n^H$. Then we can first construct local models $p_i(x)$ exhibiting the trend indicated by the LF data in the interval $[x_i^H, x_{i+1}^H]$. By doing this we do not put the whole responsibility for the trend behaviour in the weights w_i. Afterwards these local models are then blended together by suitable blending functions, such as the quadratic B-splines $B_{i-1,2}(x)$ with support $[x_{i-1}^H, x_{i+2}^H]$ and satisfying

$$\sum_{i=0}^{n-1} B_{i-1,2}(x) = 1, \qquad x_1^H \leq x \leq x_{n-1}^H$$
$$B_{i-1,2}(x_i^H) = 1/2 = B_{i-1,2}(x_{i+1}^H)$$
$$B_{i-1,2}(x_{i-1}^H) = 0 = B_{i-1,2}(x_{i+2}^H)$$

at the HF interpolation points. This leads us to the rational expression, now having a piecewise polynomial numerator and denominator, of the form

$$R_{n,w_0,\ldots,w_n}(x) = \frac{\sum_{i=0}^{n-1} w_i p_i(x) B_{i-1,2}(x)}{\sum_{i=0}^{n-1} w_i B_{i-1,2}(x)}. \tag{6}$$

Since the functions $B_{i-1,2}(x)$ are positive, it is sufficient to impose that

$$w_i > 0, \qquad i = 0, \ldots, n \tag{7}$$

to make $R_{n,w_0,\ldots,w_n}(x)$ polefree. For the local models $p_i(x)$ we use a Bézier curve, as the LF data are collected at equidistant points $x^L_{i,0} < \ldots < x^L_{i,m_i}$ in the interval $[x^H_i, x^H_{i+1}]$, with $\sum_{i=0}^{n-1}(m_i - 1) = m+1$ and where we put $x^L_{i,0} = x^H_i, x^L_{i,m_i} = x^H_{i+1}$:

$$p_i(x) = \sum_{j=0}^{m_i} f^L_{ij}\beta_{ij}(z), \tag{8}$$

$$f^L_{ij} = f\left(x^L_{i,j}\right), \qquad z = \frac{x - x^H_i}{x^H_{i+1} - x^H_i},$$

$$\beta_{ij}(z) = \binom{m_i}{j} z^j (1-z)^{m_i - j}.$$

The local polynomial model $p_i(x)$ defined on the interval $[x^H_i, x^H_{i+1}]$, has the property that it interpolates in $x^L_{i,0} = x^H_i$ and $x^L_{i,m_i} = x^H_{i+1}$ and that it follows the trend given by the so-called control points $x^L_{i,1} < \ldots < x^L_{i,m_i-1}$ inbetween. The weights in (6) are the solution of the least squares problem

$$\arg\min_{w_0,\ldots,w_n} \sum_{i=0}^{n-1}\sum_{j=0}^{m_i} \left| f^L_{i,j} - R_{n,w_0,\ldots,w_n}(x^L_{i,j})\right|^2 \tag{9}$$

or

$$\arg\min_{w_0,\ldots,w_n} \sum_{i=0}^{n-1}\sum_{j=0}^{m_i} \left| f^L_{ij} \sum_{k=0}^{n-1} w_k B_{k-1,2}(x^L_{i,j}) - \sum_{k=0}^{n-1} w_k p_k(x^L_{i,j}) B_{k-1,2}(x^L_{i,j}) \right|^2. \tag{10}$$

The sums for j running from 0 to m_i are actually sums for j from 1 to $m_i - 1$ as in the endpoints of each interval the function interpolates.

Much to our satisfaction the model (6) with (7)-(8) and (9) or (10) gives accurate results, as illustrated in Figure 4. In an upcoming paper we present more details and explain how the new technique can be generalized to the multivariate case.

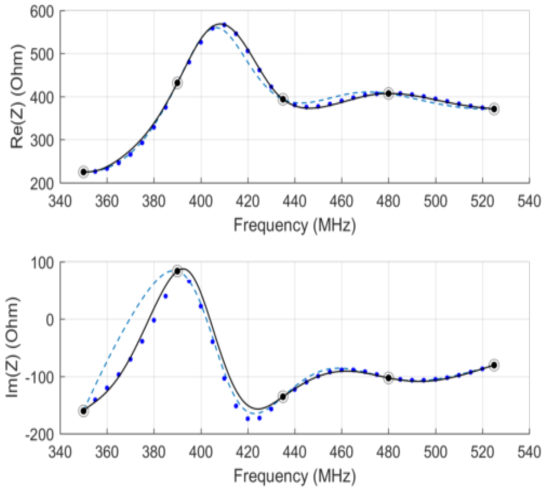

Figure 4: Blended rational interpolation of multifidelity data from (6) and (10) with (7) (circled dots: HF interpolation points, blue dots: LF data, blue dashed line: validation values, black line: rational model).

Acknowledgments

The authors acknowledge the financial support of the National Research Foundation (NRF) of South Africa, as well as that of the EUROSA project (https://www.uantwerpen.be/en/projects/eurosa/). Computations were performed using the University of Stellenbosch's HPC1 (Rhasatsha): http://www.sun.ac.za/hpc.

References

[1] R. Olsson, P.-S. Kildal, and S. Weinreb, "The eleven antenna: A compact low-profile decade bandwidth dual polarized feed for reflector antennas," *IEEE Trans. Antennas Propag.*, vol. AP-54, no. 2, pp. 368 – 375, Feb. 2006.

[2] R. Gawande and R. Bradley, "Towards an ultra wideband low noise active sinuous feed for next generation radio telescopes," *IEEE Trans. Antennas Propag.*, vol. 59, no. 6, pp. 1945–1953, Jun. 2011.

[3] N. Steenkamp, D. I. L. de Villiers, and N. Mutonkole, "Wideband pyramidal sinuous antenna for reflector antenna applications," in *European Conf. Antennas and Propagat.*, Paris, France, Mar. 2017, in press.

[4] J.-P. Berrut, "Rational functions for guaranteed and experimentally well-conditioned global interpolation," *Comput. Math. Appl.*, vol. 15, pp. 1–16, 1988.

[5] H. T. Nguyen, A. Cuyt, and O. Salazar Celis, "Comonotone and coconvex rational interpolation and approximation," *Numerical Algorithms*, vol. 58, no. 1, pp. 1–21, 2011.

[6] D. Deschrijver, T. Dhaene, O. S. Celis, and A. Cuyt, *Rational Modeling Algorithm for Passive Microwave Structures and Systems.* Berlin, Heidelberg: Springer Berlin Heidelberg, 2012, pp. 37–43.